Research on Chemical Intermediates (2023) 49:2639–2667
https://doi.org/10.1007/s11164-023-05014-6

Thio/carbohydrazone derivatives from iso(thio)/cyanates: preparation, structure elucidation, DFT studies, antimicrobial activity and DNA interactions

Muhammet Serdar Çavuş[1] · Hasan Yakan[2] · Ceren Başkan[3] · Musa Erdoğan[4] · Halit Muğlu[5]

Received: 30 December 2022 / Accepted: 4 April 2023 / Published online: 22 April 2023

Abstract

New thio/carbohydrazone derivatives (**1–10**) have been synthesized from various iso(thio)/cyanates. The chemical structures of synthesized compounds were elucidated with UV–Vis, IR, ^{1}H NMR, ^{13}C NMR spectroscopic methods, and elemental analysis. Antimicrobial activities of all synthesized compounds against Gram-positive, Gram-negative mold and yeast were screened by disc diffusion and microdilution methods. Ground state structures were obtained with the DFT approach, and also, experimental data were supported by spectroscopy calculations. In addition to calculating the reactivity parameters, intramolecular interactions and electron density distributions were analyzed and approaches to the antimicrobial properties of the compounds were presented. Furthermore, the interaction between the compounds and pBR322 plasmid DNA was investigated by gel electrophoresis. In this study to investigate the antibacterial and antifungal activity of new thio/carbohydrazone derivatives

✉ Hasan Yakan
hasany@omu.edu.tr

✉ Ceren Başkan
ceren.yavuz@amasya.edu.tr

Muhammet Serdar Çavuş
mserdarcavus@kastamonu.edu.tr

Musa Erdoğan
musa.erdogan@kafkas.edu.tr

Halit Muğlu
hmuglu@kastamonu.edu.tr

1 Department of Biomedical Engineering, Kastamonu University, Kastamonu, Turkey

2 Department of Chemistry Education, Ondokuz Mayis University, Samsun, Turkey

3 Şerefeddin Sabuncuoğlu Health Services Vocational School, Amasya University, Amasya, Turkey

4 Department of Food Engineering, Kafkas University, Kars, Turkey 36100

5 Department of Chemistry, Kastamonu University, Kastamonu, Turkey

(**1–10**), it was determined that compound **7** has a remarkable inhibitory effect on *S. aureus* (12.66 ± 1.52 mm) and compound **10** on *S. aureus* (20.33 ± 0.57 mm), *S. mutans* (16.33 ± 0.57 mm) and *A. niger* (15.33 ± 0.57 mm). The interaction results of compounds **1–10** with plasmid pBR322 DNA showed that compounds **1**, **8**, and **10** caused a reduction in the densities of form I and form II DNA. Compounds **2–7**, **9** caused a double-stranded break of plasmid DNA (Form III).

Graphical abstract

New thio/carbohydrazone derivatives have been synthesized. Structures of all compounds have been elucidated with spectroscopic approaches. Antimicrobial activities of all synthesized compounds were determined. The interaction between the compounds and pBR322 plasmid DNA was investigated by gel electrophoresis. DFT studies were performed about reactivity parameters, intramolecular interactions and electron density distributions.

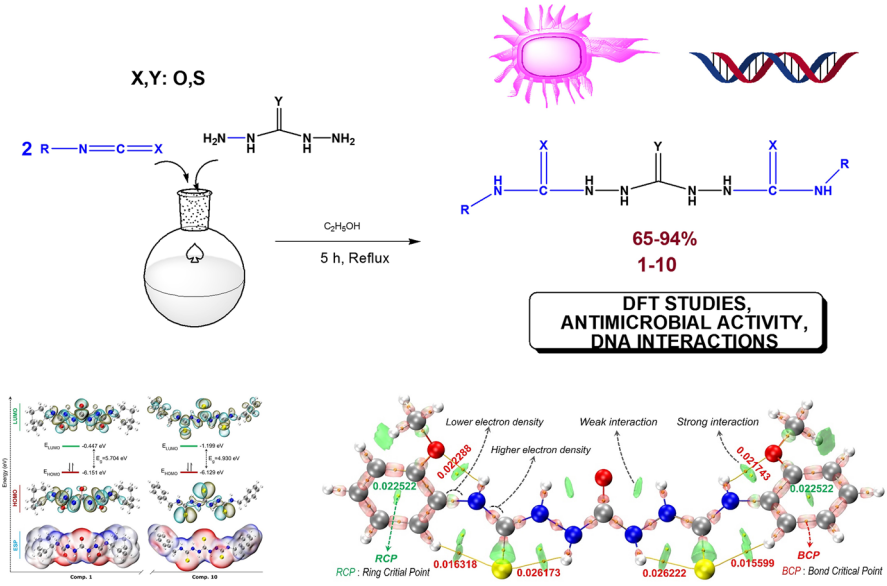

Keywords Thio/carbohydrazones · Spectroscopic studies · DFT · Antimicrobial activity · DNA interactions

Introduction

Thio/carbohydrazone and its derivatives are a significant field of organic and hetero chemistry in recent years. These compounds have many applications in pharmaceutical and biological fields such as anti-oxidant [1, 2], anti-bacterial [3], anti-fungi

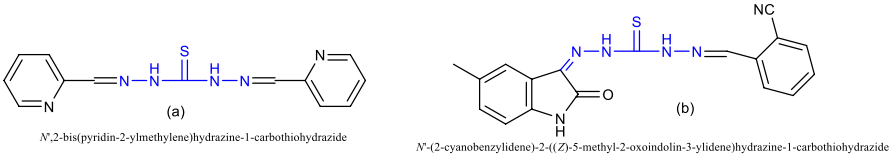

Scheme 1 Chemical structures of some antimicrobial compounds

[4], anti-microbial [5, 6], antileishmanial [7], antiviral [8], cytotoxicity [9], and anti-tumor activity [10]. In a study, *N,N'*-bis(thioamido)thiocarbohydrazone and carbohydrazone derivatives have very strong antioxidant and corrosion inhibitor activity [1]. Furthermore, mono- and bis- thiocarbohydrazone compounds with heterostructure exhibited a good antimicrobial activity against *S. aureus*, *P. aeruginosa* and *C. albicans* as shown in Scheme 1a [6]. In another study, some thiocarbohydrazones bearing 5-methylisatin scaffold exhibited moderate antimicrobial activity against *C. albicans* and *A. fumigatus* as shown in Scheme 1b [9].

The accelerating emergence of multidrug-resistant pathogens causing life-threatening infections is a worldwide concern. Infections caused by pathogens resistant to antimicrobial agents are estimated to cause 0.7 million deaths per year and are increasing rapidly daily [11]. Antibiotics used in the treatment of infections are less effective due to the increase in microbial resistance. Therefore, the development of new antimicrobial agents to combat resistant pathogens is being considered by researchers [12]. In recent years, some studies have attracted attention to investigate the interaction of newly synthesized potential antimicrobial compounds with DNA [13, 14, 15, 16, 17, 18, 19, 20].

In this study, ten thio/carbohydrazone compounds (**1–10**) were synthesized and the spectroscopic structures of the compounds (FTIR, ^{1}H, and ^{13}C NMR spectroscopic methods and elemental analysis) were characterized. Experimental results were supported by spectroscopy data obtained from density functional theory (DFT) calculations. In addition, the electronic parameters of the compounds were calculated and the effect of the substituted groups on the electronic and spectral properties of the compounds was investigated. How substituents and intramolecular interactions change electron distributions was investigated using the quantum theory of atom in molecule (QTAIM) and interaction region indicator (IRI) analyses. Furthermore, we report in vitro testing of antimicrobial activities of the synthesized compounds against four Gram-positive, four Gram-negative, and two fungi, as well as the plasmid DNA interactions of the new thio/carbohydrazone derivatives.

Experimental

Measurement and reagents

The detailed knowledge is given in Supporting Materials.

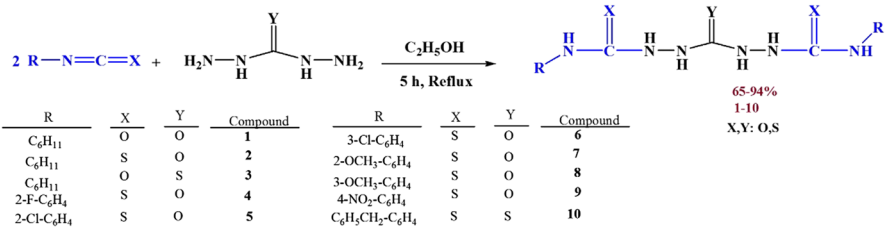

R	X	Y	Compound
C_6H_{11}	O	O	1
C_6H_{11}	S	O	2
C_6H_{11}	O	S	3
2-F-C_6H_4	S	O	4
2-Cl-C_6H_4	S	O	5

R	X	Y	Compound
3-Cl-C_6H_4	S	O	6
2-OCH_3-C_6H_4	S	O	7
3-OCH_3-C_6H_4	S	O	8
4-NO_2-C_6H_4	S	O	9
$C_6H_5CH_2$-C_6H_4	S	S	10

Scheme 2 Synthesis route of new thio/carbohydrazone derivatives (**1**–**10**)

Synthesis of thio/carbohydrazone derivatives (1–10)

In 50-mL glass flask, various iso(thio)/cyanates (10.0 mmol) and thio/carbohydrazide (5.0 mmol) in ethanol (20 mL) was refluxed at 78 °C for 5 h. The formed solid was filtered, washed, and dried in air. The compounds were successfully synthesized with good yields (65–94%) as shown in Scheme 2.

DFT calculation procedure

DFT [21, 22] calculations of the study were performed using Gaussian 09 software [23] at B3LYP/311++G(2d,2p) level of theory. The IR calculations of the compounds were successfully concluded without any imaginary frequency modes, and thus, it was checked that compounds are optimized to the ground state energies corresponding to the minimum energy points on the potential energy surface. The electronic parameters of the compounds were also obtained from the gas phase calculations at the same theory level. Using the boundary molecular orbital (FMO) energy eigenvalues, global chemical reactivity parameters such as HOMO–LUMO band gap, chemical hardness, electronegativity, electrophilic index, nucleophilic index, electroaccepting and electrodonating power were calculated. Multiwfn software [24] was used for visualization of QTAIM [24–26]and IRI [27] analyses.

In accordance with the experiments, ^{1}H and ^{13}C NMR calculations were performed in the dimethyl sulfoxide (DMSO) phase using the Gauge-independent atomic orbit (GIAO) method, with the solvent effect approximation of the conductor-like polarizable continuum model (CPCM). Relative chemical shift values were calculated by subtracting the absolute chemical shielding of tetramethylsilane (TMS), which was calculated separately at the theory level for B3LYP/6-311++G(2d,2p) (31.8149 and 183.737 ppm for ^{1}H and ^{13}C NMR, respectively).

Biological studies

Bacterial—fungal strains and growth media

The antimicrobial activities of compounds **1–10** were evaluated against four Gram-positive (*Staphylococcus aureus* ATCC®25923, *Streptococcus mutans*

ATCC®35668, *Enterococcus faecalis* ATCC®29212, *Bacillus cereus* ATCC®7064) and four Gram-negative (*Escherichia coli* ATCC®25922, *Pseudomonas aeruginosa* ATCC®27853, *Klebsiella pneumoniae* ATCC®700603, *Salmonella enteritidis* ATCC®13076) bacteria and two fungi (*Candida albicans* ATCC®10231, *Aspergillus niger* ATCC®9642). All of the bacterial and fungal strains were obtained from the Culture Collection of Ordu University Microbiology Laboratory, Turkey. Tryptic soy agar (TSA, Merck, Germany) or Tryptic soy broth (TSB, Merck, Germany) and Sabouraud Dextrose agar (SDB, Condalab, Spain) or Sabouraud Dextrose Agar (SDA, Condalab, Spain) were used for growth of bacterial and fungal cells, respectively.

Disc diffusion test

The antimicrobial activities of the new thio/carbohydrazone derivatives were measured on Mueller Hinton agar plates using Kirby-Bauer disk diffusion methods [28, 29]. Suspensions were prepared in sterile physiological saline solution (0.9%, NaCl) with bacterial and fungal concentrations of 1×10^8 cells/mL and 1×10^7 cells/mL, respectively. The prepared microorganism suspension was inoculated on Mueller Hinton Agar (MHA, Merck, Germany) with a sterile swab. Then, sterile paper discs (6 mm in diameter, Bio-analyse Ltd., Turkey) were impregnated with 20 µL (4 mg/mL) of each synthesized compound and placed on the MHA plate. Gentamicin (Bio-analyse Ltd., CN, Turkey ASD04300, 30 µg) and Ketoconazole (Bio-analyse Ltd., KTC, Turkey ASD04751, 50 µg) were used as positive controls, and dimethyl sulfoxide (DMSO, Sigma, Steinheim, Germany) was used as a negative control. After 24-h incubations at 37 °C and 27 °C for bacteria and fungi, respectively, antimicrobial activity was determined by measuring the inhibition zones using a digital caliper. It was repeated three times for all bacteria and synthesized compounds.

Microdilution test

The minimum inhibition concentration (MIC) value was determined by the microdilution method. The smallest concentration at which microbial growth is not observed is defined as the MIC value. The new thio/carbohydrazone derivatives were dissolved in dimethyl sulfoxide and then serial dilutions (4000–125 µg/mL) in cation-adjusted Mueller Hinton Broth (CAMHB) (Oxoid, Hampshire, UK) for bacteria and Sabouraud Dextrose broth for fungi were performed in a 96-well U-bottom plate. Prepared cultures were adjusted to 10^8 CFU/mL for bacteria and 10^7 CFU/mL for fungi in sterile 0.9% NaCl solution. After the bacteria were inoculated, the prepared plates were incubated for 24 h at 37 °C and 27 °C for bacteria and fungi, respectively. The smallest concentration that stopped bacterial growth after incubation was determined as the MIC value [28]. MIC value was repeated three times for all synthesized compounds.

DNA interaction test

The interactions between new thio/carbohydrazone derivatives (**1–10**) and pBR322 plasmid DNA (Thermo Fisher Scientific, USA) were studied by agarose electrophoresis. First, concentration of pBR322 plasmid DNA in Tris–EDTA (TE) buffer was adjusted (0.125 µg/µL). Then, the synthesized compounds were dissolved in DMSO at a concentration of 4000 µg/mL to prepare stock solutions. These stock solutions were diluted in decreasing concentrations (4000–250 µg/mL), and pBR322 plasmid DNA was incubated at 37 °C for 24 h. Then, aliquots of DNA/compound mixtures were loaded onto 1% agarose gel. Finally, the gel was stained with ethidium bromide and visualized under UV light [30–32].

Results and discussion

Chemical and physical properties

The results for the structure names, solubility, yields, melting points, physical properties, and elemental analyses are given in Tables 1 and 2.

Vibrational frequencies

In the FTIR spectra of the synthesized compounds (**1–10**), while the −NH stretching vibrations of vicinal amino (R−C=X) were observed at 3376–3307 cm^{-1}, the –NH stretching vibrations of thio/carbohydrazone moiety were detected at 3344–3069 cm^{-1}, respectively. The −C=O stretching vibrations were observed at 1706–1660 cm^{-1}, the −C=S signal were observed at 1457–1417 cm^{-1}, the −C–N stretching vibrations were appeared at 1314–1200 cm^{-1} (see Figs. S1–S10 in Supplementary information). For compound **4**, the −C–F stretching vibration were observed at 1115 cm^{-1}. For compounds **5** and **6**, the −C–Cl stretching vibration were observed at 1119 and 1058 cm^{-1}. For compounds **7** and **8**, the aliphatic and aromatic −C–O stretching vibrations were observed at 958, 1132 and 1023, 1226 cm^{-1}, respectively. For compound **9**, the −C–NO_2 symmetric and asymmetric vibrations were observed at 1516 and 1339 cm^{-1}, respectively. These values provided significant proofs for the products formation and the experimental/theoretical IR values of the products are presented in Table 3. The frequency data of all of the molecules are consistent with those reported for similar compounds [33–36].

^{1}H NMR interpretations

The ^{1}H NMR spectra of the compounds **1–10** having symmetrical structures were recorded in DMSO-d_6 using tetramethylsilane as the internal reference. The detailed experimental and calculated chemical shift data and coupling constants (*J*) are given in Tables 4, 5. Signals of DMSO-d_6 and water in DMSO (HOD, H_2O) were observed around 2.00, 2.55 (quintet), and 3.40 (variable, depending on the

Table 1 Structures and names, solubility, melting points, yields, and colors of the compounds

Comp.	Compounds	Solubility	Structure name	M. P. (°C)	Yields (%)	Color
1	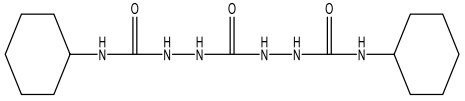	Acetone (pd) Acetonitrile (pd) Chloroform (pd) DMF (pd) DMSO (+) Ethanol (-) Ethyl acetate (pd)	2,2′-carbonylbis(*N*-cyclohexylhydrazine-1-carboxamide)	216–217	81	White
2	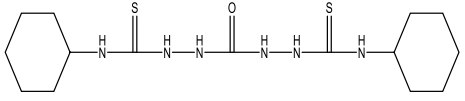	Acetone (+) Acetonitrile (pd) Chloroform (pd) DMF(+) DMSO (+) Ethanol (-) Ethyl acetate (pd)	2,2′-carbonylbis(*N*-cyclohexylhydrazine-1-carbothioamide)	217–218	76	White
3	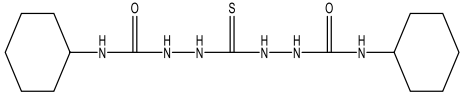	Acetone (pd) Acetonitrile (pd) Chloroform (-) DMF(pd) DMSO (+) Ethanol (-) Ethyl acetate (-)	2,2′-thiocarbonylbis(*N*-cyclohexylhydrazine-1-carboxamide)	219–220	88	White
4	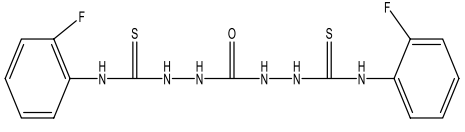	Acetone (pd) Acetonitrile (-) Chloroform (-) DMF(+) DMSO (+) Ethanol (-) Ethyl acetate (-)	2,2'-carbonylbis(*N*-(2-fluorophenyl) hydrazine-1-carbothioamide)	194–195	65	White

Table 1 (continued)

Comp.	Compounds	Solubility	Structure name	M. P. (°C)	Yields (%)	Color
5	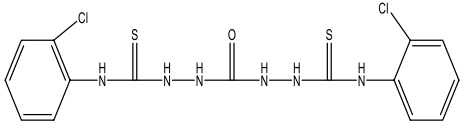	Acetone (pd) Acetonitrile (-) Chloroform (-) DMF(+) DMSO (+) Ethanol (-) Ethyl acetate (-)	2,2′-carbonylbis(*N*-(2-chlorophenyl) hydrazine-1-carbothioamide)	200–201	94	White
6	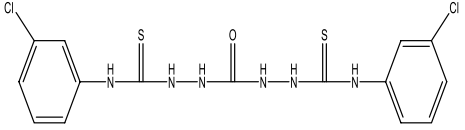	Acetone (-) Acetonitrile (-) Chloroform (-) DMF(+) DMSO (+) Ethanol (-) Ethyl acetate (-)	2,2′-carbonylbis(*N*-(3-chlorophenyl) hydrazine-1-carbothioamide)	219–210	90	White
7	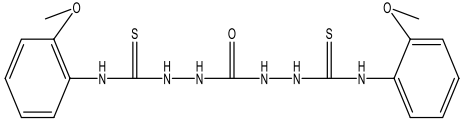	Acetone (-) Acetonitrile (-) Chloroform (-) DMF(+) DMSO (+) Ethanol (-) Ethyl acetate (-)	2,2’-carbonylbis(*N*-(2-methoxyphenyl) hydrazine-1-carbothioamide)	190–191	91	Dirty White
8	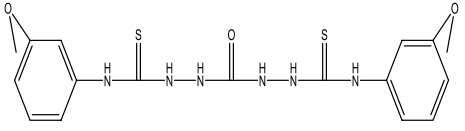	Acetone (-) Acetonitrile (-) Chloroform (-) DMF(+) DMSO (+) Ethanol (-) Ethyl acetate (-)	2,2′-carbonylbis(*N*-(3-methoxyphenyl) hydrazine-1-carbothioamide)	201–202	92	Dirty White

Table 1 (continued)

Comp.	Compounds	Solubility	Structure name	M. P. (°C)	Yields (%)	Color
9	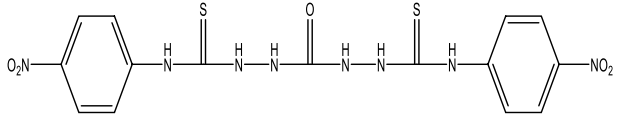	Acetone (+) Acetonitrile (-) Chloroform (-) DMF(+) DMSO (+) Ethanol (-) Ethyl acetate (-)	2,2′-carbonylbis(*N*-(4-nitrophenyl) hydrazine-1-carbothioamide)	270	87	Yellow
10	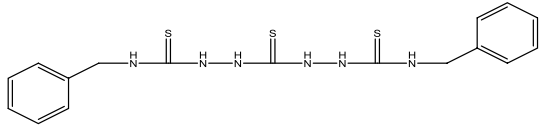	Acetone (+) Acetonitrile (+) Chloroform (-) DMF(+) DMSO (+) Ethanol (-) Ethyl acetate (pd)	2,2′-thiocarbonylbis(*N*-benzylhydrazine-1-carbothioamide)	185–186	85	White

(+): Dissolved; (-): No dissolved; (pd): Partially dissolved; DMF: *N,N*-Dimethylformamide

Table 2 Elemental analysis results of the compounds

Comp.	Molecular mass (g/mol)	Molecular formula	Calculated			Experimental		
			C%	H%	N%	(C)%	(H)%	(N)%
1	340.43	$C_{15}H_{28}N_6O_3$	52.92	8.29	24.69	53.01	8.27	24.75
2	372.55	$C_{15}H_{28}N_6OS_2$	48.36	7.58	22.56	48.29	7.57	22.60
3	356.49	$C_{15}H_{28}N_6O_2S$	50.54	7.92	23.57	50.48	7.97	23.55
4	396.43	$C_{15}H_{14}F_2N_6OS_2$	45.45	3.56	21.20	45.50	3.53	21.26
5	429.34	$C_{15}H_{14}Cl_2N_6OS_2$	41.96	3.29	19.57	42.04	3.28	19.54
6	429.34	$C_{15}H_{14}Cl_2N_6OS_2$	41.96	3.29	19.57	41.93	3.31	19.61
7	420.51	$C_{17}H_{20}N_6O_3S_2$	48.56	4.79	19.99	48.51	4.80	20.03
8	420.51	$C_{17}H_{20}N_6O_3S_2$	48.56	4.79	19.99	48.64	4.78	19.96
9	450.45	$C_{15}H_{14}N_8O_5S_2$	40.00	3.13	24.88	39.92	3.15	24.92
10	404.57	$C_{17}H_{20}N_6S_3$	50.47	4.98	20.77	50.54	5.02	20.75

solvent and its concentration) ppm, respectively [33]. In the ^{1}H NMR spectra; for all compounds, the amino peaks of the thio/carbohydrazide units (N−H1, N−H2) were resonated as a broad singlet at 10.36–7.47 ppm while the N–H3 peaks were detected at around 9.15–6.14 ppm. The protons of cyclohexyl unit (H4, H5, H6, and H7) of compounds **1–3** resonated between 1.95–0.78 ppm in the aliphatic region, as expected. On the other hand, the aromatic ring protons (H4, H5, H6, H7 and H8) of compounds **4–10** resonated in the aromatic region. For compounds **4–10**, these aromatic protons were observed 6.74–8.26 ppm. For compound **10**, the benzylic proton ($-CH_2$) signals appeared as a broad singlet at 4.72 ppm. For compound **6**, the –NH (H1), –NH (H2), and –NH (H3) proton signals of the thio/carbohydrazide moiety were observed a broad at 9.73, 9.73, and 9.03 ppm, respectively. The aromatic proton signals (H4–H8) were detected between 7.71 and 7.23 ppm as shown in Fig. 1. The H8 proton signal was observed as a singlet at 7.71 ppm. The H4 proton coupled to the H5 proton gave a doublet peak at 7.50 (d, $J=6.9$ Hz) ppm. The H5 proton coupled to the H4 and H6 protons gave a doublet peak at a triplet peak at 7.36 (t, $J=8.0$ Hz) ppm. The H6 proton coupled to the H5 proton gave rise to a doublet peak at 7.23 (d, $J=7.9$ Hz) ppm.

All other aromatic and aliphatic protons appeared in expected regions for all derivatives (see Figs. S11–S20 in Supplementary Information for spectra). The ^{1}H NMR results of all molecules are consistent with the similar compounds reported in the literature [33–36].

^{13}C NMR interpretations

The ^{13}C NMR spectra of the compounds were recorded in DMSO-d_6 (heptet peaks, 39–41 ppm) using tetramethylsilane as the internal reference. The detailed experimental and calculated chemical shift data are given in Tables 6, 7. The −C=S peaks of the thio/carbohydrazide units were observed at 180.95–184.72 ppm. For

Table 3 Experimental FTIR values of the compounds (cm^{-1})

	Comp.	R-NH	(C=Y)-NH	Ar.CH	Aliph.CH	C=O	C=S	C–N	Spec. Vib.
Experimental	**1**	3320	3150,3091	–	2930,2856	1687,1660	–	1279,1229	–
	2	3326	3193,3121	–	2980,2923	1693	1445	1258,1223	–
	3	3307	3209,3069	–	2924,2841	1682	1436	1226,1200	–
	4	3326	3191,3119	2998,2924	–	1692	1450	1260,1218	C–F:1115
	5	3329	3185	2954	–	1706	1449	1276,1232	C–Cl: 1119
	6	3346	3171	2966	–	1690	1442	1234,1208	C–Cl:1058
	7	3309	3229	2985	2841	1681	1438	1244,1219	C–O:1132, 958
	8	3311	3164	2964	2836	1701	1457	1314,1279	C–O:1226, 1023
	9	3314	3269	3078	–	1698	1451	1262,1215	NO_2:1516, 1339
	10	3376	3344, 3252	3135	2980, 2909	–	1449, 1417	1239, 1206	–
Calculated	**1**	3605.81 s, 3605.72 a	3542.32 s, 3530.34 a, 3524.47 s	–	3094.66–3011.40	1742.55 s, 1729.50 a, 1706.16 a	–	1283, 1240	–
	2	3578.09 s, 3577.97 a	3521.60 s, 3518.17 a, 3403.73 s, 3387.12 a	–	3097.97–3012.32	1702.10	1363.74	1286.23, 1253.99	–
	3	3607.65 s, 3607.56 a	3514.79 s, 3502.05 a, 3434.25 s, 3425.41 s	–	3095.77–3013.43	1730.79 s, 1724.37 a	1367.89	1242.17, 1215.11	–
	4	3577.49, 3569.54	3590.34 a, 3579.95 s, 3506.74, 3387.77	3247.17–3197.92	–	1746.87	1367.76	1261.49, 1230.44	C–F: 1199.61, 1197.23

Table 3 (continued)

Comp.	R-NH	(C=Y)-NH	Ar.CH	Aliph.CH	C=O	C=S	C–N	Spec. Vib.
5	3551.48, 3549.84	3530.91 s, 3527.30 a, 3387.22 s, 3378.98 a	3211.81–3198.46	–	1717.04	1356.58, 1355.53	1258.03, 1244.03	C–Cl: 1052.57, 1051.68
6	3584.38, 3577.95	3589.70, 3512.33, 3439.17, 3395.41	3188.80–3188.07	–	1759.36	1349.46, 1346.85	1248.25, 1239.95	C–Cl: 1098.17, 1097.87
7	3558.64, 3556.50	3521.43 s, 3518.01 a, 3383.21 s, 3374.77 a	3244.12–3196.11	3144.80–3025.95	1713.49	1361.77, 1359.44	1256.66, 1232.24	C–O: 1265.22, 1264.79, 1052.09, 1051.93
8	3586.76, 3578.57	3586.76, 3508.55, 3431.42, 3388.18	3205.70–3183.01	3141.86–3013.67	1756.87	1346.24, 1346.24	1242.81, 1225.08	C–O: 1282.58, 1282.58, 1064.82, 1064.17
9	3580.83, 3574.83	3590.09, 3510.12, 3458.37, 3399.38	3173.15–3170.91	–	1761.75	1356.27, 1349.49	1236.81, 1193.28	NO_2: 1551.53 a, 1550.18 a, 1369.20 s, 1368.50 s
10	3593.55, 3582.45	3590.04, 3391.58 a, 3370.69 s, 3366.25 a	3197.29–3165.34	3097.31–3042.47	–	1396.97, 1355.55,	1259.58, 1259.58	–

s: Symmetric stretching; a: Asymmetric stretching

Table 4 Experimental ^{1}H NMR (δ, ppm, in DMSO-d_6) values of the compounds

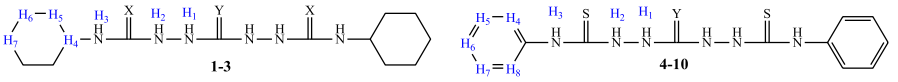

Comp.	NH, H1	NH, H2	NH, H3	H4	H5	H6	H7	H8	R
1	8.03 (bs, 2H)	7.47 (bs, 2H)	6.14 (d, J = 7.6 Hz, 2H)	1.94–1.38 (m, 2H)	1.94–1.38 (m, 8H)	1.39–0.78 (m, 8H)	1.39–0.78 (m, 4H)	–	–
2	8.95 (bs, 2H)	8.46 (bs, 2H)	7.62 (s, 2H)	1.95–1.52 (m, 2H)	1.95–1.52 (m, 8H)	1.44–0.95 (m, 8H)	1.44–0.95 (m, 4H)	–	–
3	9.36 (bs, 2H),	7.72 (bs, 2H),	6.15 (d, J = 7.3 Hz, 2H)	1.82–1.48 (m, 2H)	1.82–1.48 (m, 8H)	1.33–1.05 (m, 8H)	1.33–1.05 (m, 4H)	–	–
4	9.69 (bs, 2H)	9.46 (bs, 2H)	9.05 (s, 2H)	7.73–6.73 (m, 2H)	7.73–6.73 (m, 2H)	7.73–6.73 (m, 2H)	7.73–6.73 (m, 2H)	H8 = F	–
5	9.69 (bs, 2H)	9.51 (bs, 2H)	9.02 (s, 2H)	7.48 (dd, J = 7.9, 1.4 Hz, 2H)	7.33 (td, J = 7.7, 1.5 Hz, 2H)	7.26 (td, J = 7.8, 1.3 Hz, 2H)	7.48 (dd, J = 7.9, 1.4 Hz, 2H)	H8 = Cl	–
6	9.73 (bs, 2H)	9.73 (bs, 2H)	9.03 (s, 2H)	7.50 (d, J = 6.9 Hz, 2H)	7.36 (t, J = 8.0 Hz, 2H)	7.23 (d, J = 7.9 Hz, 2H)	H7 = Cl	7.71 (s, 2H)	–
7	9.60 (bs, 2H)	9.11 (bs, 2H)	9.11 (s, 2H)	7.97 (bs, 2H),	6.92 (t, J = 7.6 Hz, 2H)	7.15 (t, J = 7.4 Hz, 2H),	7.02 (d, J = 7.9 Hz, 2H),	H8 = OCH_3	**OCH_3:** 3.74 (s, 6H)
8	9.56 (bs, 2H)	9.56 (bs, 2H)	8.93 (s, 2H)	7.33–7.03 (m, 2H)	7.33–7.03 (m, 2H)	6.74 (dd, J = 8.4, 2.0 Hz, 2H)	H7 = OCH_3	7.33–7.03 (m, 2H)	**OCH_3:** 3.72 (s, 6H)
9	10.00 (bs, 2H)	10.00 (bs, 2H)	9.15 (s, 2H),	7.97 (d, J = 8.6 Hz, 4H	8.26 (d, J = 9.0 Hz, 4H),	H6 = NO_2	8.26 (d, J = 9.0 Hz, 4H),	7.97 (d, J = 8.6 Hz, 4H	–
10	10.36 (bs, 1H), 9.88 (s, 1H)	9.55 (bs, 1H), 9.33 (s, 1H)	8.86 (s, 1H), 8.20 (s, 1H)	7.55–7.02 (m, 2H)	7.55–7.02 (m, 2H)	7.55–7.02 (m, 2H)	7.55–7.02 (m, 2H)	7.55–7.02 (m, 2H)	**CH_2:** 4.72 (bs, 4H)

Table 5 Theoretical ^{1}H NMR (ppm, in DMSO) values of the compounds

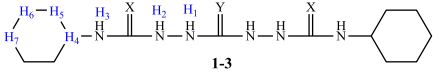

1-3

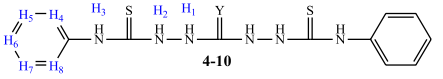

4-10

Comp.	NH, H1	NH, H2	NH, H3	H4	H5	H6	H7	H8	R
1	6.11 (2H)	5.80 (2H)	4.09 (2H)	4.09 (2H)	2.00–1.17 (8H)	1.78–1.54 (8H)	1.49–1.46 (4H)	–	–
2	6.47 (2H)	6.65 (2H)	5.29 (2H)	4.71 (2H)	2.12–1.1.28 (8H)	179–1.62 (8H)	1.49–1.47 (4H)	–	–
3	7.05 (2H)	6.05 (2H)	4.24 (2H)	4.10 (2H)	2.01–1.23 (8H)	1.78–1.59 (8H)	1.49–1.47 (4H)	–	–
4	9.38, 6.50	8.78, 7.39	7.37, 7.24	8.21, 8.20	7.61 (2H)	7.68, 7.60 (2H)	7.58, 7.55(2H)	H8 = F	–
5	6.58, 6.51 (2H)	7.36, 7.33 (2H)	7.34, 7.20 (s, 2H)	8.25, 8.10 (2H)	7.70, 7.69 (2H)	7.77, 7.61 (2H)	7.94, 7.85 (2H)	H8 = Cl	–
6	6.78, 6.66 (2H)	7.27, 7.13 (2H)	7.41, 7.38 (2H)	8.02, 8.00 (2H)	7.80, 7.73 (2H)	7.67, 7.65 (2H)	H7 = Cl	7.40, 7.36 (2H)	–
7	6.56, 6.48 (2H)	7.25, 7.21 (2H)	8.01, 7.77 (2H)	8.90, 8.64 (2H)	7.35, 7.32 (2H)	7.64, 7.58 (2H),	7.35, 7.31 (2H)	H8 = OCH_3	**OCH_3:** 4.34–3.85 (6H)
8	6.72, 6.60 (2H)	7.25, 7.17 (2H)	7.59, 7.38 (2H)	7.47, 7.46 (2H)	7.72, 7.65 (2H)	7.23, 7.23 (2H)	H7 = OCH_3	6.94, 6.81 (2H)	**OCH_3:** 4.17–3.78 (6H)
9	9.29, 6.72(2H)	8.97, 7.35 (2H)	7.93, 7.50 (2H)	9.32, 7.22 (2H)	8.79, 8.75 (2H)	H6 = NO_2	8.85, 8.79 (2H)	9.02, 7.51 (2H)	-
10	10.51, 7.05 (2H)	9.67, 6.89(2H)	5.36, 5.27 (2H)	7.87, 7.65(2H)	7.94, 7.81 (2H)	7.86, (2H)	7.92, 7.88 (2H)	7.88, 7.84 (2H)	**CH_2:** 5.03-4.31(4H)

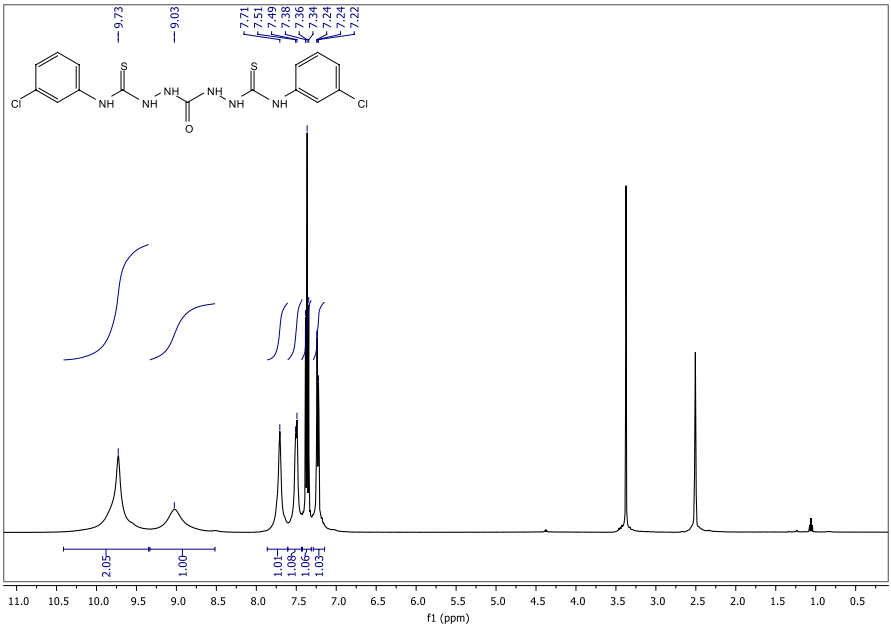

Fig. 1 ^{1}H NMR spectrum of compound **6** (400 MHz, DMSO-d_6)

all compounds, the C1 and C2 carbon (–C=S or –C=O) peaks were detected at 156.39–184.72 ppm as shown in Fig. 2. The carbons of cyclohexyl unit (C3, C4, C5, and C6) of compounds **1–3** resonated between 52.73 and 24.48 ppm in the aliphatic region, as expected. On the other hand, the aromatic ring carbons (C3–C8) of compounds **4–10** resonated in the aromatic region. For compound **10**, the benzylic carbon ($-CH_2$) signals appeared at 46.87 ppm. For the compounds **7–8**, the characteristic OCH_3 carbons resonated at 55.68 and 55.06 ppm, respectively. All other aromatic and aliphatic carbons appeared in expected regions for all derivatives (see Figs. S21–S30 in Supplementary Information for details). For compound **6**, the –C=O (C1) signal of the carbohydrazide moiety was observed at 156.44 ppm, and the characteristic –C=S (C2) peak of thiourea unit was observed at 181.19 ppm. The carbon atoms (C3–C8) of the aryl ring were detected at 140.48, 124.49, 132.23, 124.70, 129.68, and 123.28 ppm, respectively. The C3 and C5 aromatic carbon signals were observed at 140.48 and 132.23 ppm. These carbon signals were downfield shifted due to the presence of the nitrogen and chloride atom, respectively. The NMR data are in very good agreement with the structure of the compounds. The ^{13}C NMR values of all compounds are consistent with the similar compounds reported in the literature [33–36].

Table 6 Experimental ^{13}C NMR (δ, ppm, in DMSO-d_6) values of the compounds

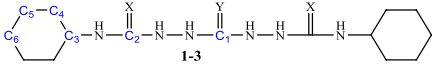

1-3

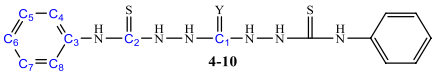

4-10

Comp.	C1	C2	C3	C4	C5	C6	C7	C8	R
1	157.94	159.03	48.10	33.00	24.60	25.28	–	–	–
2	156.70	181.27	52.73	32.06	24.79	25.21	–	–	–
3	156.95	184.72	48.13	32.90	24.48	25.27	–	–	–
4	156.46	182.57	123.90 (d, J = 3.3 Hz),	158.40–158.05 (m)	115.67 (d, J = 19.9 Hz)	128.30–127.60 (m)	130.66–129.79 (m)	126.88 (d, J = 11.7 Hz)	–
5	156.47	182.29	136.44	129.25	127.84	130.66	126.97	130.77	–
6	156.44	181.19	140.48	124.49	132.23	124.70	129.68	123.28	–
7	157.02	181.08	125.07	151.62	111.31	127.58	119.70	125.82	**OCH_3**: 55.68
8	156.62	180.95	140.31	110.50	159.01	116.98	140.06	128.83	**OCH_3**: 55.06
9	156.39	180.99	145.42	123.94	123.94	143.26	123.94	123.94	-
10	181.82	184.46	138.92	127.15	127.99	126.61	127.99	127.15	**CH_2**: 46.87

Table 7 Theoretical ^{13}C NMR (ppm, in DMSO) values of the compounds

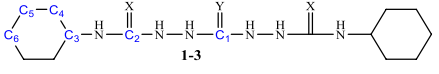

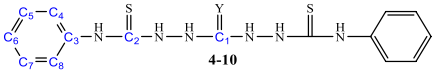

Comp.	C1	C2	C3	C4	C5	C6	C7	C8	R
1	166.05	164.32	49.67	32.53, 30.61	24.34, 23.40	22.83	–	–	–
2	165.24	191.22	55.04	32.12, 28.90	24.10, 23.34	22.52	–	–	–
3	195.25	163.72	49.64	32.77, 30.55	24.33, 23.48	22.77	–	–	–
4	161.88	192.47, 179.46	132.49	165.68, 164.34	120.95, 120.55	133.52, 131.78	129.23, 129.01	135.18, 132.94	–
5	165.26	192.67, 192.06	141.90, 141.70	143.48, 141.18	135.66, 135.51	133.93, 133.24	132.23, 132.14	137.50, 135.54	–
6	165.55	193.24, 192.66	146.53, 146.31	129.89, 129.76	148.30, 147.92	132.06, 132.03	135.09, 135.06	132.68, 132.37	–
7	165.39	190.09, 189.34	133.26, 132.57	158.24, 157.73	114.29, 115.00	131.22, 130.77	123.80, 123.75	129.32, 127.63	**OCH_3**: 58.01, 57.37
8	165.85	193.63, 192.80	146.85, 146.27	111.91, 110.35	169.16, 168.90	120.64, 120.41	134.82, 134.66	126.46, 125.38	**OCH_3**: 57.13, 57.05
9	161.28	190.87, 176.17	153.81, 152.61	127.81, 124.73	133.18, 132.60	150.82, 148.87	131.73, 131.63	126.04, 125.16	-
10	184.47	191.06, 182.40	143.99, 143.39	137.09, 136.88	134.97, 134.94	134.73, 134.67	135.14, 134.17	136.68, 136.21	**CH_2**: 54.85, 54.01

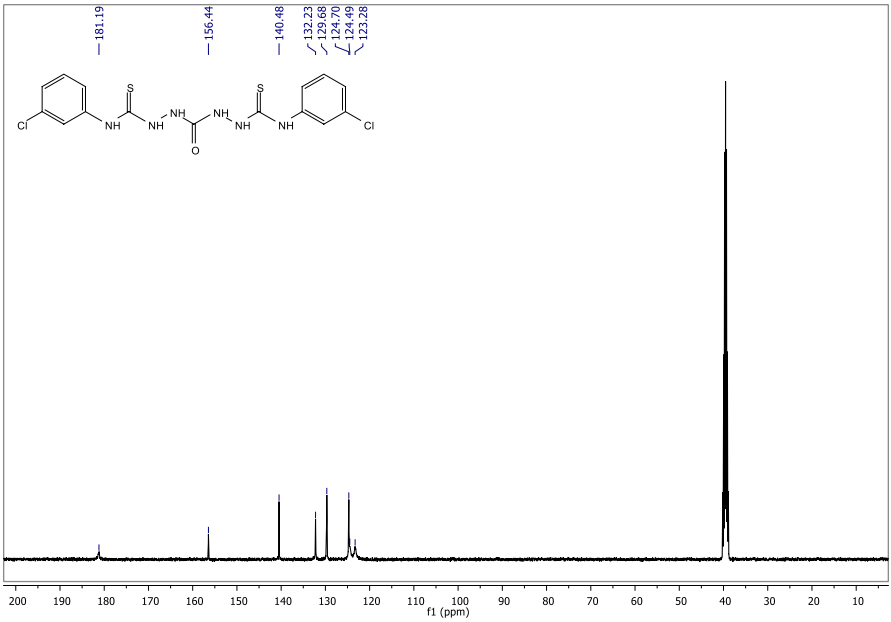

Fig. 2 ^{13}C NMR spectrum of compound **6** (100 MHz, DMSO-d_6)

UV–Vis interpretations

The electronic absorption spectra of the synthesized compounds (**1**–**10**) demonstrated that absorption bands of all products were exhibited range from 210 to 800 nm in dimethylsulfoxide (see in Figs. S31–S40). The electronic spectra of these compounds show remarkable absorption bands of aromatic ring (C=C) and thio/carbohydrazone (C=S, C=O) region owing to transitions of a $\pi \rightarrow \pi^*$ and an $n \rightarrow \pi^*$. Except for compounds **1–3**, the $\pi \rightarrow \pi^*$ type transitions of C=C on the aromatic ring are seen at 255.9 nm. This transition is characteristic benzenoid (B) band of aromatic structure [37]. While the $n \rightarrow \pi^*$ transitions of the C=O double bond were assigned at 243.2–260.7 nm for all compounds, the bands at 261.7–347.7 nm were observed to the electronic transition $n \rightarrow \pi^*$ of the thiocarbohydrazone moiety (C=S). The electronic spectral data of the all compounds are summarized in Table 8. These values are in agreement with the results that reported similar compounds [38, 39].

DFT analysis

The calculated electronic parameters of the compounds may allow us to make some assumptions about their reactivity. In a rough approximation, we can say that the smaller the HOMO–LUMO energy gap, E_g, of a compound, the lower its kinetic stability or the higher its tendency to react (see Fig. 3 for a demonstration on compound

Table 8 Electronic spectral data (nm) of all the compounds (1–10) in DMSO

Compound	$\pi \rightarrow \pi^*$, B band	$n \rightarrow \pi^*$, C=O	$n \rightarrow \pi^*$, C=S
1	–	260.7	–
2	–	250.0	261.7
3	–	247.1	261.7
4	255.9	247.1	272.4
5	255.9	243.3	277.3, 287.9
6	255.9	243.2	274.4
7	255.9	243.2	264.6, 291.8
8	255.9	247.1	271.4
9	255.9	257.8	296.6, 347.7
10	255.9	–	271.4

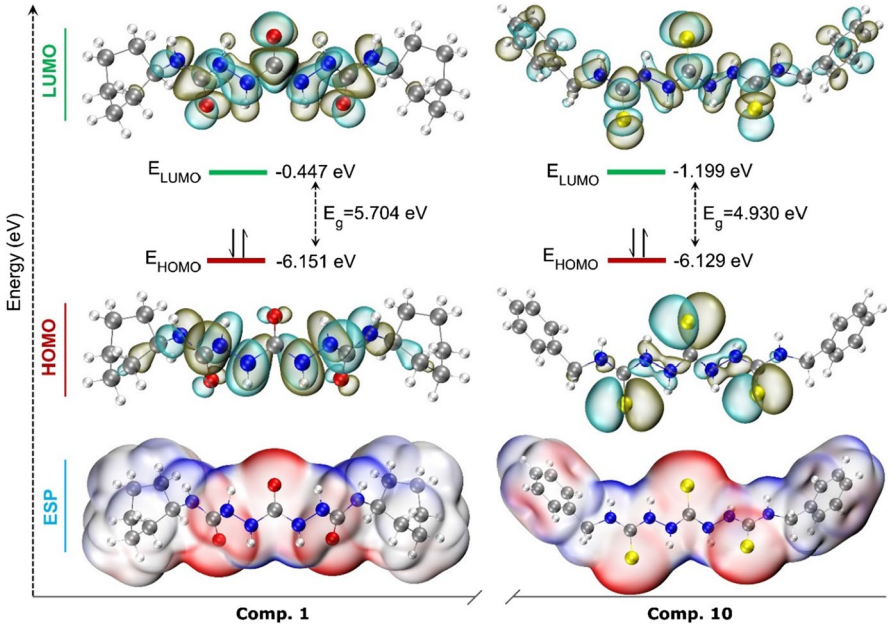

Fig. 3 ESP, HOMO and LUMO surface of compounds **1** and **10**

1 and **10**; see Fig. S41 in Supplementary information for all compounds). In this context, compounds **1–3** with higher E_g values than other compounds are expected to show lower reactivity. Consistent with the experimental results, it can be said that the activities of compounds **1–3** were weaker than the other compounds in general of the test bacterial strains. Among these three compounds, it is seen that especially compound **1** is more reactive against Gram-positive bacteria, albeit weakly. In these compounds, which do not contain any substituents on the cyclohexane structure, it can be said that the oxygen atoms in the structure of compound **1** are one of the

triggering parameters of this reactivity. Considering compounds **1**–**3**, the presence of sulfur atom in compound **3** appears to play a role in reducing the activity on Gram-positive species (see Table 10). An electronegativity-enhancing effect of sulfur is observed in compounds **1**–**3**: compound **1** had the lowest electronegativity, while compound **2** with more sulfur was calculated the highest. In the other group, the electronegativity values of compounds **4**–**10** were higher (see Table 9).

The shift of the substituents from the *ortho* position to the *meta* position (compounds **5** and **6**; **7** and **8**) caused both HOMO and LUMO energies of the compounds to decrease, which corresponds to a more electrophilic behavior of the compounds. In accordance with this expectation, the electrophilic indices of the *meta*-substituted compounds were also calculated larger, or in other words, the nucleophilic indices were calculated smaller. The calculated electronic parameters of *p*-NO_2-substituted compound **9** differed markedly from those of the other compounds. This compound with the smallest E_g value has the largest both electronegativity and electrophilic index. In addition to being high in electron accepting and electron donating power values, it showed reactivity almost only against fungi species (except *S. enteritidis*). Although compound **10** had the highest antimicrobial effect compared to other compounds, electronic parameter values obtained from FMO eigenvalues did not show any significant deviation from those of other compounds.

The electron distribution of a compound is not a static variable and is sensitively dependent on conformation and intra/intermolecular interactions. In addition to determining the physical and chemical properties of the compound, it can enable us to make some predictions about the behavior of the compound in chemical reactions and, accordingly, its biological activity. At this point, it should be noted that these parameters alone are far from being used as determinants of the dynamics of a reaction mechanism.

Figure 4 gives some QTAIM data including the IRI surfaces of compound **7**, as well as electron densities in RCPs and BCPs.

The electron density of the cyclohexane structure in compounds **1**–**3** in RCP and in BCP of C−C bonds was calculated to be lower than that of all other compounds. In addition, it was observed that the sulfur atom enters the intramolecular interactions more than the oxygen atom and exhibits stronger intramolecular interactions (see Supplementary Fig. S42 for all compounds). This interaction increases the delocalization of electrons and as a result changes the electron density distribution on the compound. It can be predicted that weaker bound electrons, which are delocalized through intramolecular interactions, will be easier to participate in the reaction processes. The electron densities of (N)H−(C)S and (N)H−(N)H bonds in BCP are higher in compound **10** than in other compounds, and the electron density between S−N(H) is lower. These data strengthen the possibility that reactions to antibacterial and fungal species are concentrated around the central skeleton of the compounds. Besides, the more freely dihedral rotation of the benzyl group may also enable it to perform conformational changes that will facilitate reactions more easily and be less affected by steric effects.

Compounds **4**–**9** differ among themselves only in terms of substituted groups, and in general, these compounds are not reactive to Gram-negative bacterial strains. *o*-F-substituted compound **4** and *o*-Cl-substituted compound **5**, which showed reactivity

Table 9 Calculated electronic parameters of the compounds

Comp.	*E* (au)	E_{HOMO} (eV)	E_{LUMO} (eV)	ΔE (eV)	η (eV)	χ (eV)	ω (eV)	ε (eV)	α *(au)*	μ *Debye*	ω^+ (eV)	ω^- (eV)
1	− 1143.030	− 6.151	− 0.447	5.704	2.852	3.299	1.908	3.344	242.136	3.200	0.018	3.317
2	− 1788.937	− 6.074	− 0.788	5.286	2.643	3.431	2.227	3.421	292.219	5.171	0.059	3.490
3	− 1465.985	− 6.090	− 0.682	5.408	2.704	3.386	2.120	3.405	270.074	2.005	0.043	3.429
4	− 1980.22	− 6.362	− 1.518	4.844	2.422	3.940	3.205	3.133	301.235	2.347	0.238	4.178
5	− 2700.929	− 6.420	− 1.623	4.797	2.399	4.022	3.371	3.075	340.052	2.924	0.275	4.296
6	− 2700.928	− 6.498	− 1.679	4.819	2.410	4.089	3.469	2.997	335.628	3.327	0.292	4.381
7	− 2010.805	− 5.955	− 1.307	4.648	2.324	3.631	2.837	3.540	353.048	6.983	0.184	3.815
8	− 2010.801	− 6.072	− 1.398	4.674	2.337	3.735	2.985	3.423	342.234	4.857	0.209	3.944
9	− 2190.820	− 6.974	− 3.020	3.954	1.977	4.997	6.315	2.521	362.911	3.418	1.153	6.150
10	− 2183.290	− 6.129	− 1.199	4.930	2.465	3.664	2.723	3.366	346.822	4.198	0.146	3.810

E Energy; ΔE:$E_{LUMO} - E_{HOMO}$; η: Chemical hardness; χ : Electronegativity; ω: Electrophilic index; ε: Nucleophilic index; α: Polarizability; μ: Dipole moment; ω^+: electroaccepting power; ω^-: electrodonating power

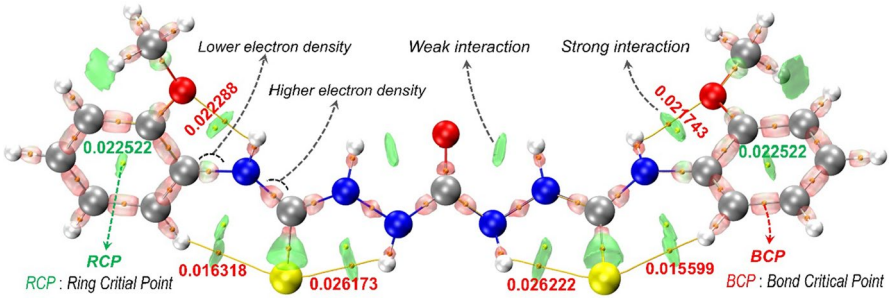

Fig. 4 IRI surface of intramolecular interaction. QTAIM data of electron density (e/bohr^3) on RCP and BCP of compound **7**

against fungal species, also showed reactivity against *S. aureus*. The stronger participation of the chlorine atom in the intramolecular interactions than the fluorine atom is expected to increase electron delocalization and therefore the reactivity of the compound is expected to be higher, which has been experimentally shown that compound **5** has slightly higher antimicrobial reactivity than compound **4** (see Table 10).

Although experimental studies of antimicrobial activities and DNA interactions of compounds have a wide field of study in the literature, the effectiveness of DFT calculations in understanding the biological activities of compounds has not reached a remarkable point yet. The calculations are mostly based on the determination of the geometric and electronic properties of the synthesized compounds [40–46], and the relationship of the calculated electronic data with the biological reactivity properties of the compounds could not be clarified. Since electronic data are obtained from the single states of the compounds, the effects of intermolecular interactions on the conformations cannot be taken into account, and the thermodynamic variables of the reaction processes cannot be determined and kept constant, it is not possible to talk about the absolute accuracy of the predictions regarding a reaction. The usability of electronic parameters can be improved by evaluating and testing the predictions or assumptions made as a reference for newly synthesized compounds. For this, it is inevitable to make experiments and calculations on more compounds.

Biological studies

Antimicrobial studies

The antimicrobial activities of the new thio/carbohydrazone derivatives (**1–10**) were determined by disc diffusion and microdilution method. The results are shown in Table 10. It was determined that DMSO used as solvent control did not have any antimicrobial effect (>4000 µg/mL). Among the tested compounds, especially compound **10** exhibited good activity against Gram-positive bacteria *S. aureus* (20.33 ± 057 mm) and *S. mutans* (16.33 ± 0.57 mm) when compared with the positive control antibiotic. Compound **10** showed moderate antibacterial activity (15.33 ± 0.57 mm) against *S. enteritidis* among Gram-negative bacteria. In addition, compound **10** demonstrated

Table 10 Antimicrobial activities of compounds, disc diffusion method (mm, mean ± std) and MIC values (μg /mL)

Test microorganisms										
Comp.	Bacteria								Fungus	
	Gram positive				Gram negative				Yeast	Mold
	S. aureus	*S. mutans*	*E. faecalis*	*B. cereus*	*E. coli*	*P. aeruginosa*	*K. pneumoniae*	*S. enteritidis*	*C. albicans*	*A. niger*
1	10.33 ± 1.33	10.33 ± 1.33	9.66 ± 0.57	-	-	-	-	9.33 ± 0.57	-	-
	2000	2000	4000	> 4000	> 4000	> 4000	> 4000	2000	> 4000	> 4000
2	-	-	-	9.00 ± 0.00	-	-	-	-	-	-
	> 4000	> 4000	> 4000	4000	> 4000	> 4000	> 4000	> 4000	> 4000	> 4000
3	9.00 ± 0.00	-	-	-	-	-	-	-	-	-
	4000	> 4000	> 4000	> 4000	> 4000	> 4000	> 4000	> 4000	> 4000	> 4000
4	9.33 ± 0.57	-	-	-	-	-	-	-	9.33 ± 0.57	10.33 ± 1.15
	4000	> 4000	> 4000	> 4000	> 4000	> 4000	> 4000	> 4000	4000	2000
5	9.00 ± 0.00	-	-	14.33 ± 1.52	-	-	-	-	9.66 ± 0.57	11.00 ± 1.00
	4000	> 4000	> 4000	2000	> 4000	> 4000	> 4000	> 4000	4000	2000
6	-	9.33 ± 0.57	-	-	-	-	-	-	-	-
	> 4000	4000	> 4000	> 4000	> 4000	> 4000	> 4000	> 4000	> 4000	> 4000
7	12.66 ± 1.52	10.66 ± 0.57	10.33 ± 0.57	10.33 ± 1.33	-	9.00 ± 0.00	-	-	-	-
	2000	2000	2000	2000	> 4000	4000	> 4000	> 4000	> 4000	> 4000
8	11.33 ± 1.15	-	9.33 ± 0.57	13.33 ± 0.57	-	-	-	-	-	-
	2000	> 4000	4000	2000	> 4000	> 4000	> 4000	> 4000	> 4000	> 4000
9	-	-	-	-	-	-	-	13.66 ± 1.15	12.00 ± 0.53	10.33 ± 0.57
	> 4000	> 4000	> 4000	> 4000	> 4000	> 4000	> 4000	2000	2000	2000
10	20.33 ± 0.57	16.33 ± 0.57	-	11.33 ± 1.15	13.00 ± 1.73	10.33 ± 1.33	-	15.33 ± 0.57	12.66 ± 1.52	15.33 ± 0.57
	250	1000	> 4000	2000	2000	2000	> 4000	1000	2000	1000

Table 10 (continued)

Test microorganisms										
Comp.	Bacteria								Fungus	
	Gram positive				Gram negative				Yeast	Mold
	S. aureus	*S. mutans*	*E. faecalis*	*B. cereus*	*E. coli*	*P. aeruginosa*	*K. pneumoniae*	*S. enteritidis*	*C. albicans*	*A. niger*
DMSO	-	-	-	-	-	-	-	-	-	-
	>4000	>4000	>4000	>4000	>4000	>4000	>4000	>4000	>4000	>4000
CN	21.00±0.00	17.66±0.57	19.33±1.57	15.00±1.00	23.66±0.57	28.33±1.52	25.33±1.15	23.66±0.57	NT	NT
	<125	<125	<125	<125	<125	<125	<125	<125		
KTC	NT	NT	NT	NT	NT	NT	NT	NT	15.33±0.57	20.33±1.52
									1000	<125

DMSO: Dimethyl sulfoxide; NT: Not tested, (-): Inhibition zone did not occur; CN: Gentamicin (30 µg); KTC: Ketoconazole (50 µg)

moderate effect against *C. albicans* (12.66 ± 1.52 mm) and *A. niger* (15.33 ± 0.57 mm). Therefore, compound **10** from thio/carbohydrazone derivatives was determined to be the most effective compound in this study. Compound **7** showed moderate antibacterial activity against Gram-positive bacteria used in the study. On the other hand, compound **7** displayed low activity against only *P. aeruginosa* from Gram-negative bacteria. Compound **9** demonstrated moderate activity against *C. albicans* (12.00 ± 0.53 mm) and *A. niger* (10.33 ± 0.57 mm). Compounds **5** and **8** showed moderate inhibitory activity against *B. cereus* (respectively, 14.33 ± 1.52 and 13.33 ± 0.57 mm). On the other hand, compounds **2**, **3** and **6** indicated slight activity against tested microorganisms. MIC values for control (DMSO) are > 4000 µg/mL. It is seen that this value is 250 µg/mL for compound **10** against *S. aureus*. As seen in Table 10, MIC values for compound **10** against *S. mutans*, which is Gram-positive bacteria, were 1000 µg/mL, while it was 1000 µg/mL for *S. enteritidis*, which is Gram-negative bacteria. Moreover, compound **10** has antifungal activity and the MIC for *A. niger* was determined to be 1000 µg/mL. These results show that the new thio/carbohydrazone derivatives have antimicrobial activity against some microorganisms. In previous studies on this subject, it has been found that these compounds with similar structures have significant antimicrobial activities [47, 48]. According to these literature studies, it has been determined that these synthesis compounds have an inhibitory effect on *S. aureus*. Similarly, in the present study, especially compound **10** showed significant antibacterial effect on *S. aureus*.

DNA and compound interactions

DNA interaction studies damage and conformational change due to the binding of syntheses and plasmid DNA are determined by gel electrophoresis. The conformational change in DNA has been interpreted considering the conversion of supercoiled DNA (Form I) to open circular DNA (Form II) and linear DNA (Form III) [49, 50]. Therefore, in this study, we used the agarose gel electrophoresis method to determine whether the synthesized compounds (**1–10**) cause conformational changes on plasmid DNA. Figure 5 shows the separation of pBR322 plasmid DNA on gel after incubation with different concentrations of compounds between 4000 and 250 µM.

As seen in Fig. 5, according to the result of Gel electrophoresis, lane 1 used as plasmid control presented two bands for untreated plasmid DNA. Lane 2 and Lane 3 represent TRIS–EDTA and DMSO control, respectively. Lane 4–8 refers to plasmid DNA incubated with compounds ranging from 4000 to 250 µg/mL. In Fig. 5, compounds **2–7**, **9** appear to have DNA nuclease activity that converts supercoiled Form I DNA to linear Form III DNA. Compounds **1**, **8** and **10** caused a decrease in the densities of Form I and Form II DNA.

Conclusion

Ten new thio/carbohydrazone derivatives (**1–10**) have been synthesized and isolated in good yields with 65–94%. The structures of these new compounds have been elucidated by UV–Vis, FTIR, ^{1}H, and ^{13}C NMR spectroscopy, and elemental analysis.

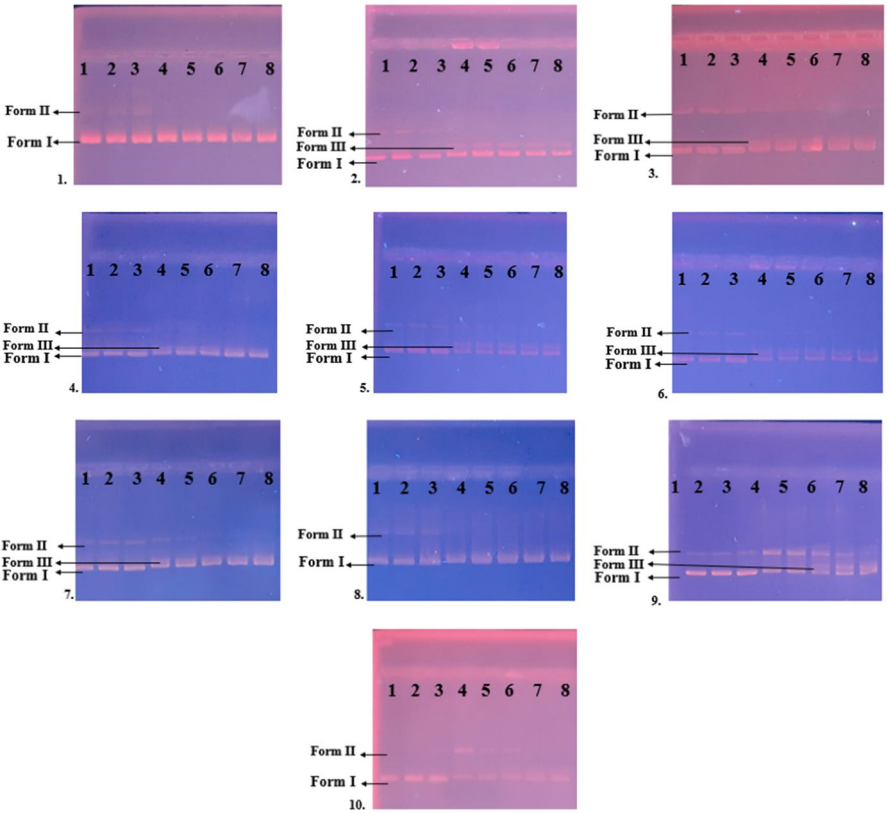

Fig. 5 Agarose gel electrophoresis pattern of the interaction of pBR322 plasmid DNA and different concentrations of synthesized compounds **(1–10)**. (Lane 1: untreated plasmid DNA, Lane 2: Tris EDTA control, Lane 3: DMSO control, Lanes 4–8: DNA treated by compounds at the different concentration as 4000, 2000, 1000, 500 and 250 µg/mL

To support the experimental spectroscopic data of the compounds, DFT calculations were performed and good agreement was observed between them. Although the CPCM approach was used for solvent effects, deviations in the hydrogen chemical shift values due to atoms with high electronegativity in ^{1}H NMR data naturally arose because the intermolecular interactions could not be fully reflected in the calculations. It was observed that the sulfur atom exhibits stronger intramolecular interactions than the oxygen atom. In this way, it can be said that the delocalization of electrons increases and it will be easier for weakly bound delocalized electrons to participate in the reaction processes. It can also be further tested experimentally that the free dihedral rotation of the benzyl group may be a property that will facilitate reactions.

The antimicrobial activities of all the compounds were evaluated against four Gram-positive (*S. aureus*, *S. mutans*, *E. faecalis*, *B. cereus*), four Gram-negative (*E. coli*, *P. aeruginosa*, *K. pneumoniae*, *S. enteritidis*) bacterial strains using gentamicin

as a positive control and two fungal strains (*C. albicans*, *A. niger*) using ketoconazole as positive controls. We found that compound **10**, one of the new thio/carbohydrazone derivatives compounds, showed promising antibacterial activities (20.33 ± 0.57 mm, MIC values = 250 µg/mL) especially against *S. aureus* from Gram (+) bacteria. It has also been observed that this compound has a moderate antifungal effect on *A. niger* (15.33 ± 0.57 mm, MIC values = 1000 µg/mL). In addition, compounds **2–7**, **9** were determined to have a strong interaction with pBR322 plasmid DNA.

Supplementary Information The online version contains supplementary material available at https://doi.org/10.1007/s11164-023-05014-6.

Acknowledgements The DFT calculations reported in this paper were partially performed at TUBITAK ULAKBIM, High Performance and Grid Computing Center (TRUBA resources). We would like to thank Dr. Seyhan Ozturk at Ondokuz Mayıs University for taking the UV-Vis spectra.

Author contributions MSÇ: Theoretical Calculations, Writing–Review. HY: Spectroscopic Characterization, Writing–Review, Visualization & Editing. CB: Biological studies, Writing–Review. ME: Spectroscopic Characterization, Writing–Review. HM: Synthesis, Characterization, Writing–Review. All authors reviewed the manuscript.

Funding This research did not receive any specific grant from funding agencies in the public, commercial, or not-for-profit sectors.

Data availability The results/data/figures in this manuscript have not been published elsewhere, nor are they under consideration by another publisher.

Declarations

Conflict of interest The authors declare that they have no conflict of interest a financial or personal nature.

Ethical approval All of the material is owned by the authors, and/or no permissions are required.

References

1. M.S. Çavuş, H. Yakan, C. Özorak, H. Muğlu, T.K. Bakır, Res. Chem. Intermed. **48**, 1593 (2022)
2. H. Muğlu, B.Z. Kurt, F. Sönmez, E. Güzel, M.S. Çavuş, H. Yakan, J. Phys. Chem. Solids **164**, 110618 (2022)
3. Z.H. Chohan, H. Pervez, K.M. Khan, C.T. Supuran, J. Enzyme Inhib. Med. Chem. **20**, 81 (2005)
4. G.B. Bagihalli, P.G. Avaji, P.S. Badami, S.A. Patil, J. Coord. Chem. **61**, 2793 (2008)
5. K. El-Mahdy, A. El-Kazak, M. Abdel-Megid, M. Seada, O. Farouk, Acta Chim. Slov. **63**, 18 (2016)
6. A.R. Božić, S.K. Bjelogrlić, I.T. Novaković, N.R. Filipović, P.M. Petrović, A.D. Marinković, T.R. Todorović, I.N. Cvijetić, ChemistrySelect **3**, 2215 (2018)
7. M.T. Muhammad, N. Ghouri, K.M. Khan, M.I. Choudhary, S. Perveen, Med. Chem. **14**, 725 (2018)
8. K. Gangarapu, S. Manda, A. Jallapally, S. Thota, S.S. Karki, J. Balzarini, E. De Clercq, H. Tokuda, Med. Chem. Res. **23**, 1046 (2014)
9. M.T. Gabr, N.S. El-Gohary, E.R. El-Bendary, N. Ni, M.I. Shaaban, M.M. El-Kerdawy, Synth. Commun. **48**, 2899 (2018)
10. M. Sathisha, V. Revankar, K. Pai, Met. Based Drugs **2008** (2008)
11. K. Fink, M. Uchman, Coord. Chem. Rev. **431**, 213684 (2021)

12. G. Elmacı, H. Duyar, B. Aydıner, I. Yahaya, N. Seferoğlu, E. Şahin, S.P. Çelik, L. Açık, Z. Seferoğlu, J. Mol. Struct. **1184**, 271 (2019)
13. A. Bolhuis, J.R. Aldrich-Wright, Bioorg. Chem. **55**, 51 (2014)
14. M. Kumar, V. Kumar, V. Beniwal, Med. Chem. Res. **24**, 2862 (2015)
15. A. Okumuş, G. Elmas, A. Binici, B. Aydın, L. Açık, Z. Kılıç, T. Hökelek, Inorg. Chim. Acta **538**, 121001 (2022)
16. A.M. Abu-Dief, R.M. El-Khatib, F.S. Aljohani, H.A. Al-Abdulkarim, S. Alzahrani, G. El-Sarrag, M. Ismael, Comput. Biol. Chem. **97**, 107643 (2022)
17. I.J. Simpson, M. Lee, A. Kumar, D.W. Boykin, S. Neidle, Bioorg. Med. Chem. Lett. **10**, 2593 (2000)
18. M. Chemchem, I. Yahaya, B. Aydıner, N. Seferoğlu, O. Doluca, N. Merabet, Z. Seferoğlu, Tetrahedron **74**, 6897 (2018)
19. R. Mehandi, R. Arif, M. Rana, S. Ahmedi, R. Sultana, M.S. Khan, M. Maseet, M. Khanuja, N. Manzoor, N. Nishat, J. Mol. Struct. **1245**, 131248 (2021)
20. P. Mondal, P. Sengupta, U. Pal, S. Saha, A. Bose, Spectrochim. Acta Part A Mol. Biomol. Spectrosc. **245**, 118936 (2021)
21. P. Hohenberg, W. Kohn, Phys. Rev. **136**, B864 (1964)
22. W. Kohn, L.J. Sham, Phys. Rev. **140**, A1133 (1965)
23. M.J. Frisch, G. Trucks, H. Schlegel, G. Scuseria, M. Robb, J. Cheeseman, G. Scalmani, V. Barone, B. Mennucci, G. Petersson et al., *Gaussian 09 (Revision A.02)* (Gaussian Inc., Wallingford, 2009)
24. T. Lu, F. Chen, J. Comput. Chem. **33**, 580 (2012)
25. R.F. Bader, Acc. Chem. Res. **18**, 9 (1985)
26. R.F. Bader, Chem. Rev. **91**, 893 (1991)
27. T. Lu, Q. Chen, Chem. Methods **1**, 231 (2021)
28. C. Clsi, Clin. Lab Stand. Inst. **35**, 16 (2016)
29. Ö. Ertürk, Biologia **61**, 275 (2006)
30. H. Akbaş, A. Okumuş, Z. Kılıç, T. Hökelek, Y. Süzen, L.Y. Koç, L. Açık, Z.B. Çelik, Eur. J. Med. Chem. **70**, 294 (2013)
31. N. Asmafiliz, Z. Kılıç, A. Öztürk, Y. Süzen, T. Hökelek, L. Açık, Z.B. Çelik, L.Y. Koc, M.L. Yola, Z. Üstündağ, Phosphorus SulfurSilicon Relat. Elem. **188**, 1723 (2013)
32. S. Pawar, A. Amate, D. Chakravarty, R.J. Butcher, A.A. Kumbhar, J. Chem. Sci. **133**, 1 (2021)
33. H. Muğlu, H. Yakan, A.G.A. Misbah, M.S. Çavuş, T.K. Bakır, Res. Chem. Intermed. **47**, 4985 (2021)
34. H. Yakan, T.K. Bakır, M.S. Çavuş, H. Muğlu, Res. Chem. Intermed. **46**, 5417 (2020)
35. H. Muğlu, H. Yakan, T.K. Bakir, Turk. J. Chem. **44**, 237 (2020)
36. G. Kiran, M. Sarangapani, T. Gouthami, A.R. Narsimha Reddy, Toxicol. Environ. Chem. **95**, 367 (2013)
37. B. Sharma, *Instrumental Methods of Chemical Analysis, Krishna Prakashan Media* (Goel Publishing House, Meerut, 2000)
38. K.H.D. Reddy, S.-M. Lee, K. Seshaiah, R.K. Babu, J. Serb. Chem. Soc. **78**, 229 (2013)
39. G. Subhashree, J. Haribabu, S. Saranya, P. Yuvaraj, D.A. Krishnan, R. Karvembu, D. Gayathri, J. Mol. Struct. **1145**, 160 (2017)
40. N. Kurita, K. Kobayashi, Comput. Chem. **24**, 351 (2000)
41. S. Niroomand, M. Khorasani-Motlagh, M. Noroozifar, S. Jahani, A. Moodi, J. Mol. Struct. **1130**, 940 (2017)
42. S. Singhal, P. Khanna, L. Khanna, Heliyon **5**, e02596 (2019)
43. M. Erol, I. Celik, G. Kuyucuklu, J. Mol. Struct. **1234**, 130151 (2021)
44. M. Salihović, M. Pazalja, S.Š Halilović, E. Veljović, I. Mahmutović-Dizdarević, S. Roca, I. Novaković, S. Trifunović, J. Mol. Struct. **1241**, 130670 (2021)
45. N. Chouchène, A. Toumi, S. Boudriga, H. Edziri, M. Sobeh, M.A. Abdelfattah, M. Askri, M. Knorr, C. Strohmann, L. Brieger, Molecules **27**, 582 (2022)
46. S. Farooq, Z. Ngaini, A.I. Daud, W.M. Khairul, Polycycl. Aromat. Compd. **42**, 5422 (2022)
47. H.M. Metwally, N.A. Khalaf, E. Abdel-Latif, M.A. Ismail, BMC Chem. **17**, 1 (2023)
48. M.B. Muluk, P.S. Phatak, S.B. Pawar, S.T. Dhumal, N.N. Rehman, P.P. Dixit, P.B. Choudhari, K.P. Haval, J. Chin. Chem. Soc. **66**, 1507 (2019)

49. N. Asmafiliz, Z. Kılıc, A. Öztürk, T. Hökelek, L.Y. Koc, L. Açık, O.Z.L. Kısa, A. Albay, Z. Üstündağ, A.O. Solak, Inorg. Chem. **48**, 10102 (2009)
50. G.D. Çelik, A. Dişli, Y. Öner, L. Açık, Chem. Pharm. Bull. **60**, 578 (2012)